OPEN ACCESS
Energy Storage ARTICLE

Carnot battery with thermochemical energy storage and supercritical CO_2 power cycle: Thermodynamic and techno-economic characteristics

Huawei Liu,[2] Yongqing Zhang,[1] Qianghui Xu,[1,*] Wei Han,[3] Kezhen Zhang,[3] Xiao Yang,[3] Chenglong Yang,[3] Sheng Li,[1] and Jun Shen[1]
*Correspondence: xuqh12@bit.edu.cn
Received: January 28, 2026; Accepted: April 20, 2026; Published Online: April 23, 2026; https://doi.org/10.59717/j.xinn-energy.2026.100163

GRAPHICAL ABSTRACT

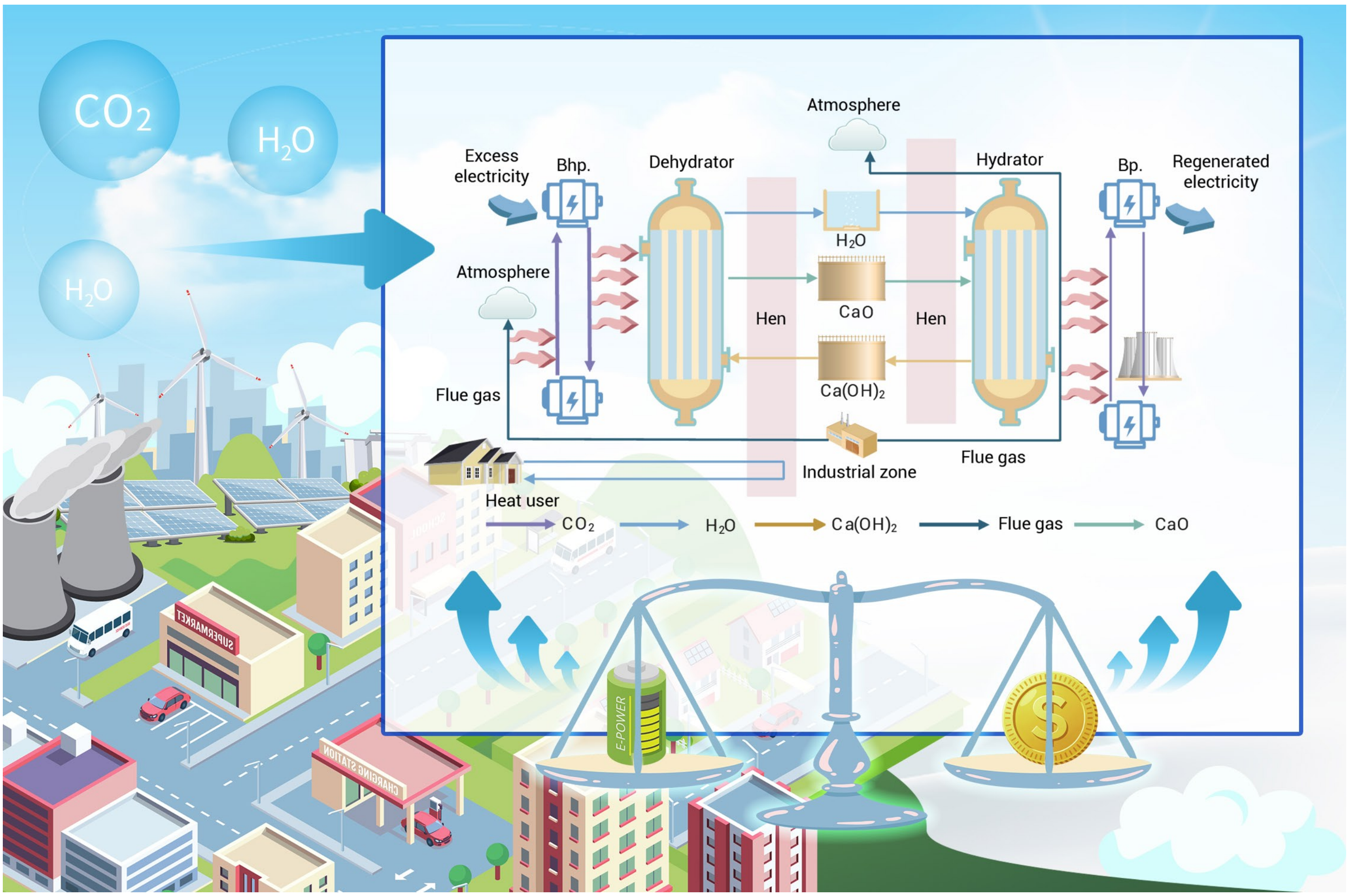

PUBLIC SUMMARY

- A $Ca(OH)_2$/CaO-based Carnot battery with S-CO_2 cycles and waste heat recovery is proposed.
- Multi-objective optimization achieves 67.95% round-trip efficiency and 1.200 RMB/kWh LCOE.
- Scaling from 10 MW to 50 MW reduces LCOE by 46.3% and doubles IRR to 13.64%.
- Materials influence system economics mainly via the unit price–design cycle life ratio.
- Profitability mainly depends on discharge pricing; high TPC remains the main challenge.

Carnot battery with thermochemical energy storage and supercritical CO_2 power cycle: Thermodynamic and techno-economic characteristics

Huawei Liu,[2] Yongqing Zhang,[1] Qianghui Xu,[1,*] Wei Han,[3] Kezhen Zhang,[3] Xiao Yang,[3] Chenglong Yang,[3] Sheng Li,[1] and Jun Shen[1]

[1]School of Mechanical Engineering, Beijing Institute of Technology, Beijing 100081, China

[2]Key Laboratory of Power Station Energy Transfer Conversion and System of MOE, School of Energy Power and Mechanical Engineering, North China Electric Power University, Beijing 102206, China

[3]Xi'an Thermal Power Research Institute Co., Ltd. Xi'an 710032, China

*Correspondence: xuqh12@bit.edu.cn

Received: January 28, 2026; Accepted: April 20, 2026; Published Online: April 23, 2026; https://doi.org/10.59717/j.xinn-energy.2026.100163

Citation: Liu H., Zhang Y., Xu Q., et al. (2026). Carnot battery with thermochemical energy storage and supercritical CO_2 power cycle: Thermodynamic and techno-economic characteristics. *The Innovation Energy* **3**:100163.

The global transition toward decarbonized energy systems necessitates efficient long-duration energy storage solutions to address renewable intermittency. Conventional technologies face limitations in scalability, safety and geography, highlighting the promise of Carnot batteries. This study proposes a novel Carnot battery system integrating calcium hydroxide/calcium oxide thermochemical energy storage, supercritical CO_2 Brayton heat pump and power cycles, and industrial waste heat recovery. Through multi-objective optimization using the NSGA-II algorithm and HEATSEP framework, the system achieved a round-trip efficiency of 67.95% and a LCOE of 1.200 RMB/kWh at 50 MW scale—placing it at a high level among current Carnot battery systems. Sensitivity analyses confirm robust scalability: when scaling from 10 MW to 50 MW, the LCOE decreases by 46.3% and the IRR increases from 6.79% to 13.64%. Furthermore, increasing the annual operating hours to 2560 h significantly reduces the LCOE while substantially raising the IRR. For high-cost materials, extending cycle life can yield 21.47% reduction in LCOE. Critically, system profitability is governed by discharge revenue. In markets with modest price differentials, economic feasibility therefore depends on additional reductions in capital cost, such as implementing deep integration with existing coal-fired assets. This integrated system and optimization directions provide a practical, generalizable blueprint for near-term, cost-competitive Carnot batteries.

INTRODUCTION

The global energy system is undergoing a rapid transition toward decarbonization and renewable integration, driven by significant growth of wind and solar power installations.[1,2] However, the inherent intermittency and volatility of these renewable sources pose significant challenges to grid stability,[3,4] necessitating large-scale, long-duration energy storage (LDES) technologies, which is a key resource in enabling zero-emissions electricity grids.[5]

In LDES, such long-duration storage capabilities are fundamentally unattainable for electrochemical systems because they were unable to prevent their self-discharge problem.[6] Conversely, physical storage alternatives like pumped hydro[7,8] and compressed air energy storage[9] (CAES) face insurmountable geographical and infrastructural barriers.[10] Chemical energy storage pathways have also been widely investigated for LEDS. Among these, hydrogen energy storage and power-to-gas (PtG) technologies convert surplus electricity into chemical fuels through electrolysis and subsequent synthesis processes, offering advantages of high energy density and compatibility with existing natural gas infrastructure. However, their overall round-trip efficiencies are typically limited due to multiple energy conversion steps, including electrolysis, gas compression or synthesis, storage, and reconversion to electricity. In addition, the deployment of hydrogen or synthetic fuels often requires dedicated transport, storage, and safety infrastructure, which can significantly increase the technical requirements, economic costs, and regulatory complexity of the system.[11-13] These limitations have catalyzed a paradigm shift toward Carnot battery systems.[14] Carnot batteries—a class of electro-thermal-electric storage systems based on thermodynamic cycles—have emerged as a pivotal solution due to their high energy density, geographical flexibility, and compatibility with industrial waste heat recovery.[15]

Existing Carnot battery energy storage technologies can be categorized into four types based on their cycle classifications:[16] Brayton cycle heat pump energy storage,[17,18] Rankine cycle heat pump energy storage,[19,20] liquid air energy storage[21,22](LAES), and other Carnot battery concepts.[23] Among these, comparative analyses of three candidate cycles—organic Rankine, steam Rankine, and supercritical CO_2 (S-CO_2) Brayton—reveal that S-CO_2-based systems achieve higher round-trip efficiency in thermochemical energy storage (TCES) applications, primarily due to the system's compact turbomachinery and operation near the critical point.[24,25] LAES is a novel large-scale energy storage solution based on cryogenic technology. However, its application in long-duration energy storage scenarios is constrained by thermal losses that occur over time during heat/cold storage processes.[22]

The core innovation of Carnot batteries resides in their adaptive thermal cycle architecture, which enables integration with advanced energy storage mechanisms. Recent studies prioritize thermodynamic optimization through synergistic integration of TCES materials (e.g., $CaO/Ca(OH)_2$) with S-CO_2 Brayton cycles.[26-29] This hybrid approach capitalizes on S-CO_2's high cycle efficiency[24] (45–55%) while leveraging TCES's intrinsic capacity for high-temperature[27,29] (>400°C) energy retention—a critical advantage for long-duration energy storage applications. TCES can achieve energy densities of 500–1500 kJ/kg under ideal conditions through reversible solid-gas reactions,[30] This combination of high-density storage positions TCES-embedded Carnot batteries as a promising alternative for renewable energy integration, particularly in scenarios requiring both frequency regulation and seasonal load shifting.

Meanwhile, $Ca(OH)_2/CaO$ has emerged as one of the benchmark TCES material, offering reaction enthalpy of 104 kJ/mol and low material cost.[28] Additionally, Liu et al. quantified energy storage capacity and reversibility over 20 cycles,[31] while Leander et al.[32] conducted an energy storage experiment with a capacity of 0.5 kW and 40.5 storage cycles. Despite these advancements, current research disproportionately focuses on material-level optimization, with critical gaps persisting in system-scale integration strategies and lifecycle cost modeling. Crucially, the techno-economic performance of such hybrid systems—particularly levelized cost of storage (LCOS)—is influenced by multiple factors including material properties, capital expenditures, and operational strategies. A systematic sensitivity analysis is urgently required to quantify the marginal effects of critical parameters and guide engineering optimization.

Building upon prior work[29] on $CaO/Ca(OH)_2$-S-CO_2 integrated Carnot batteries, this study proposes an economic sensitivity analysis by introducing economic objectives and an NSGA-II algorithm, and we explore optimal trade-offs among energy efficiency, exergy efficiency, and cost. This research addresses three key innovations:

(1) Establishing a closed-loop energy conversion pathway of "electricity-heat pump-$Ca(OH)_2$ storage/S-CO_2 power generation" to overcome efficiency limitations of conventional Carnot batteries;

(2) Developing a life-cycle cost model integrated with sensitivity analysis to elucidate economic responses to material costs, annual operating hours,

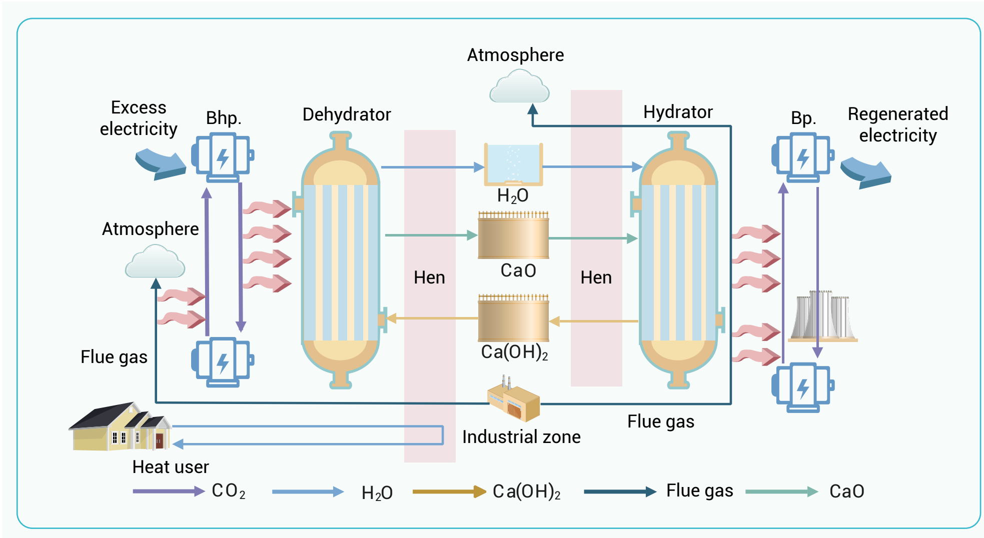

Figure 1. Conceptual schemes of the proposed $Ca(OH)_2/CaO$ Carnot battery system powered by excess electricity.

system scale and electricity price fluctuations;

(3) Delivering a technically viable and economically competitive solution for long-duration renewable energy storage.

Our findings aim to bridge the gap between theoretical innovation and practical implementation, offering actionable insights for engineering design, policy incentives, and market-driven deployment of Carnot battery technology, thereby accelerating the global transition to a low-carbon energy future.

MATERIALS AND METHODS

The carnot battery system based on TCES

The schematic diagram of the proposed Carnot battery system (Figure 1) illustrates a sequential energy conversion chain, integrating five key components from left to right: (1) an electricity-to-heat heat pump coupled with industrial waste heat recovery, (2) a thermochemical dehydration reactor, (3) chemical energy storage tanks, (4) a hydration reactor for chemical-to-thermal energy conversion, and (5) a thermal-to-electricity power cycle. This horizontal layout emphasizes the unidirectional energy flow and modularity of the system, aligning with the principles of energy cascade utilization and long-duration storage.

A detailed description of the calcium-based composite assumption, the S-CO_2 BHP–TCES system configuration, waste-heat-assisted heat exchange network, and operating constraints of the hydration/dehydration reactors is provided in Note S1.

Simulation models

Steady-state thermodynamic models were implemented to simulate the mass and energy balances of all system components. A customized in-house thermodynamic program was developed to solve the coupled heat transfer and chemical reaction processes, ensuring numerical stability and convergence under varying operational conditions. The thermophysical properties of gaseous and liquid working fluids (e.g., S-CO_2, water/steam) were retrieved from the NIST REFPROP database, while the thermodynamic data for solid reactants (CaO, $Ca(OH)_2$) were sourced from the Aspen Plus V11 property library, ensuring consistency with widely accepted industrial standards. The key parameters and governing formulations of the S-CO_2 Brayton heat pump (BHP)/Brayton cycles, $Ca(OH)_2/CaO$ reactors, heat exchange networks, and the associated energy and exergy models are comprehensively documented in Note S1.2.

For the scope of this study, the capital costs of major system components are incorporated, and the total initial investment cost is calculated as the sum of individual component costs. In addition to annual operating costs (including operation, maintenance, and interest rate costs, which are proportional to the total system cost), material replacement due to cyclic deactivation of energy storage materials is categorized as external resource expenditures. All costs are adjusted to 2024 values using the Chemical Engineering Plant Cost Index (CEPCI), and final economic metrics are reported in Chinese Yuan (RMB), assuming a USD-RMB exchange rate of 7.2492. The detailed capital and operating cost models for the S-CO_2 turbomachinery, heat exchangers, heat exchange network, auxiliary equipment, and the definitions of total plant cost (TPC) and total annual cost (TAC) are comprehensively presented in Note S2.

Technical assessments

An intuitive performance indicator of the proposed system is the energy efficiency, defined as the ratio of the regenerated electricity and useful heat supply to the total input of excess electricity and low-temperature industrial waste heat over the complete charging–discharging cycle. To further account for energy quality degradation, the exergy efficiency is evaluated in parallel, providing a more rigorous thermodynamic measure of system effectiveness. The round-trip efficiency is used to characterize the technical performance of the Carnot battery, quantifying the fraction of stored electrical energy that can be recovered during discharge. From an economic perspective, the levelized cost framework is adopted to assess electricity generation costs by incorporating the total capital investment, annual operating expenditures, and the discount rate over the system lifetime. In addition, the IRR is employed to evaluate investment profitability, corresponding to the discount rate at which the net present value (NPV) becomes zero, while the DPP is introduced as a risk-oriented indicator that explicitly accounts for the time value of money. The detailed definitions and calculation methods of all these performance metrics are provided in Note S3.

Optimization method

The Carnot battery system coupled with TCES exhibits strong multidimensional coupling among thermodynamic cycle efficiency, reaction kinetics, material costs, and equipment lifetime. Single-objective optimization risks critical trade-offs: pursuing thermodynamic efficiency may necessitate expensive materials or complex processes, elevating the LCOE and compromising economic viability; conversely, minimizing LCOE could select inefficient storage media or cycle equipment, substantially degrading energy efficiency and round-trip efficiency. Consequently, this section establishes a Pareto frontier through multi-objective optimization to quantify the round-trip efficiency versus LCOE trade-off, providing scientific basis for system parameterization. The system scale is extended from 1 MW[29] to 50 MW with a uniform minimum heat exchange temperature approach of 15°C for techno-economic co-optimization. Reference operating parameters include: 8-hour charge/discharge cycles, 320 annual cycles (2560 operational hours/year), energy storage utilizing curtailed electricity incurs zero cost. Considering the combined effects of bulk energy storage (energy arbitrage), transmission-and-distribution (T&D) support, and frequency regulation, the sale price is approximated by the peak-period tariff (1.000–1.800 RMB/kWh); in the base case we set 1.591 RMB/kWh. The energy storage material exhibits a maximum effective cycle number of 50 and a unit price of 1500 RMB/t. The multi-objective optimization workflow, algorithm configuration, and physical constraints are comprehensively detailed in Note S4.

Validation

The credibility of the proposed Carnot battery system is established through a component-level validation strategy, supported by reliable performance and cost data.

The operational reliability of the core power cycle—specifically, the reversible Brayton cycle encompassing the compressor, turbine, and key heat exchangers—has been directly demonstrated in prior work.[29,33] The validation involved benchmarking against reliable literature data, including both simulation and experimental results, which confirmed the accuracy of the models

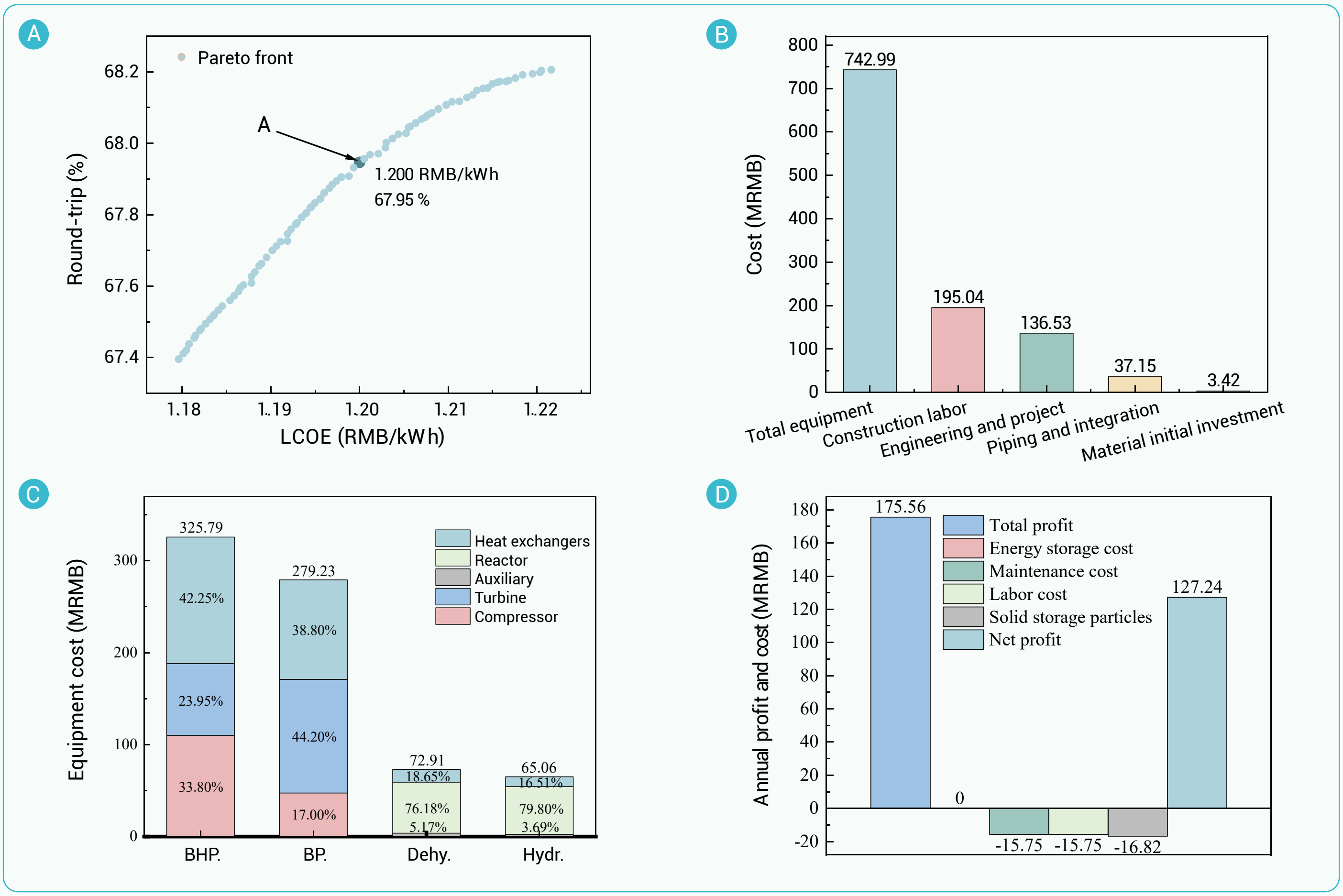

Figure 2. Multi-objective optimization results and techno-economic performance of the Carnot battery system (A) Pareto front of the multi-objective optimization; (B) breakdown of total initial investment; (C) distribution of subsystem equipment costs; (D) annualized cost and profit structure.

for these critical components. Furthermore, the configuration of the heat exchanger network and the reactor is directly adopted from the well-established design detailed in Ref. [27].

The cost models for the entire system are grounded in substantial industrial data. The cost correlations for each component within the supercritical CO_2 cycle are derived from a comprehensive analysis of between 4 to 24 individual supplier quotations.[34] Cost data for the heat exchanger network and reactor were also sourced from Ref. [27].

By building upon these foundational elements with proven performance and economically credible cost data, the overall system-level analysis presented in this work is positioned on a highly reliable and validated foundation.

RESULTS

This section focuses on the multi-objective optimization of the Carnot battery system, aiming to reveal synergies and trade-offs among system parameters by balancing thermodynamic efficiency and economic metrics. Leveraging the NSGA-II construct the Pareto frontier depicting round-trip efficiency versus Levelized Cost of Electricity (LCOE) to quantify energy-cost conflicts. The influence of critical parameters on equipment cost proportions and operational revenue is investigated through system scaling to the 50 MW scale. Parametric sensitivity studies further investigate dynamic impacts of material costs, cycle life, annual operating hours, and unit scale on LCOE. Commercial viability is evaluated by incorporating regional electricity pricing policies. Finally, we propose scaled deployment strategies for high price-differential regions through dynamic payback period and Internal Rate of Return (IRR) models.

System optimization results—base case

The base case is designed to showcase the upper limit of the performance of the proposed Carnot battery system under relatively ideal conditions. These ideal conditions primarily involve the use of almost pure $Ca(OH)_2$ particles and medium-temperature flue gas. In practical applications, achieving 100% purity of $Ca(OH)_2$ is challenging. Therefore, the base case assumes a mass fraction of 98% $Ca(OH)_2$ in particles, with the remaining fraction consisting mainly of a single impurity. The industrial waste flue gas for the low-temperature heat source of the S-CO_2 BHP cycle is set to operate at a temperature of 300°C. In this work, a medium-sized Carnot battery system is analyzed with a charging electrical power of 50 MW. Following optimization via the NSGA-II algorithm, the final results presented in Figure 2A demonstrate a negative correlation between round-trip efficiency and LCOE along the Pareto frontier. Targeting an optimal energy-economic compromise solution, design point A in the Figure 2A was selected based on equal weighting, the optimized parameters include the pre-optimized expansion pressure in the S-CO_2 Brayton power (BP) cycle's $P_{dis,BPFT}$ = 16.28 MPa, determined through subsystem-level pre-optimization, and the maximum BHP system pressure of 17.32 MPa, intermediate pressure of 12.30 MPa, With this configuration corresponding to zero electricity pricing during energy storage periods, the Carnot battery round-trip efficiency is 67.95%, and the LCOE is 1.200 RMB/kWh.

As illustrated in Figure 2B, the total equipment cost constitutes 66.65% of the total investment in the Carnot battery system, representing the dominant expenditure component. This cost is significantly higher than the sum of all other costs, most of which scale proportionally with the equipment cost. Compared to 50 MW-class power plants or other energy storage facilities, the direct equipment cost of 742.99 million RMB is notably high, which corresponds to the equipment cost after applying the total system cost factor (i_{TASC} = 1.13), with the actual total initial investment reaching 1.26 billion RMB.

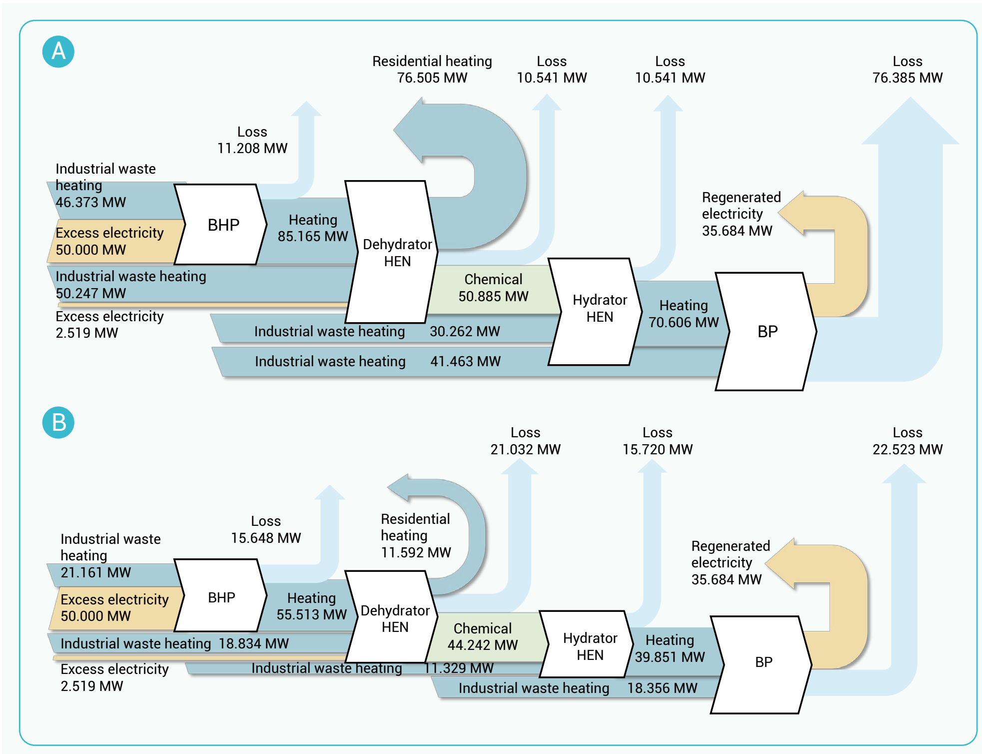

Figure 3. Multi-objective optimization results of Carnot battery system (A) Energy flow diagram (B) Exergy flow diagram.

The reactor costs constitute a significantly higher proportion of the total investment compared to other components. Specifically, the dehydrator reactor cost represents 55.54 MRMB, accounting for 76.18% of its relevant section, while the hydration reactor cost is 51.88 MRMB, representing 79.80%. In contrast, the heat exchanger network and auxiliary equipment costs contribute substantially less to the overall expenditure. Critically, the significant investment in heat exchangers pervasive across all major modules highlights the paramount importance and cost impact of thermal management within Carnot battery technology.

Furthermore, the economic viability of the Carnot battery system requires a comprehensive assessment considering both the initial investment and the full lifecycle operating costs. As shown in Figure 2D, under optimized parameters, the annual profit and cost breakdown of the Carnot battery system are depicted. Within the annual operating expenditure, the electricity storage cost is eliminated due to the design utilizing zero electricity pricing. Material consumption constitutes a significant portion of the expenditure, amounting to 16.82 million RMB. Additionally, maintenance cost and labor cost, which are proportional to the initial investment, represent other major components of the operating costs. Based on an annual renewable electricity generation of 91.35 GWh and a realized electricity revenue of 1.591 RMB/kWh, coupled with a heating revenue standard of 42.84 RMB/GJ, the annual net profit reaches approximately 127.24 million RMB.

Figure 2C delineates the equipment cost breakdown for the Carnot battery system, revealing pronounced heterogeneity in capital expenditure allocation across its primary functional modules. Notably, the BHP cycle incurs the highest equipment costs at approximately 325.79 MRMB. These costs are dominated primarily by heat exchangers, accounting for 42.25% of the total due to higher recuperative power requirements, followed by compressors at 33.80%, while turbines constitute a smaller share of 23.95% owing to their lower power contribution. Conversely, the BP cycle incurs significantly lower equipment costs of approximately 279.23 MRMB, within this cost structure, heat exchangers maintain a comparable proportion to the BHP system at approximately 38.80%. However, a key difference emerges within the BP cost structure: turbine costs rise substantially to dominate at 44.20%, while compressor contributions are markedly lower, constituting only 17.00% of the total. This pronounced disparity between the turbine and compressor cost shares originates primarily from the fundamental power relationship inherent in their respective Brayton cycle configurations. Specifically, within the reverse Brayton cycle employed by the BHP cycle, compressor power significantly exceeds turbine power. Conversely, in the forward Brayton cycle typical of BP system, turbine power output substantially surpasses compressor power.

As shown in Figure 3A&B, the system achieves an energy efficiency of 50.80% and an exergy efficiency of 38.68%, with the heat exchanger network configuration identical to that in Reference.[29] The system integrates excess electricity and industrial waste heat through the BHP and the heat exchanger network, enabling an effective cascade utilization of multi-grade energy. The total input energy is partially upgraded to high-temperature heat to drive the dehydration reactor, resulting in a chemical energy storage rate of 50.885 MW, while additional low- and medium-temperature heat is recovered to supply residential heating. Meanwhile, the stored chemical energy is released during the hydration process and converted back to electricity via the power block, yielding 35.684 MW of regenerated electricity. Overall, the energy flow diagram indicates that a considerable fraction of the input energy is delivered

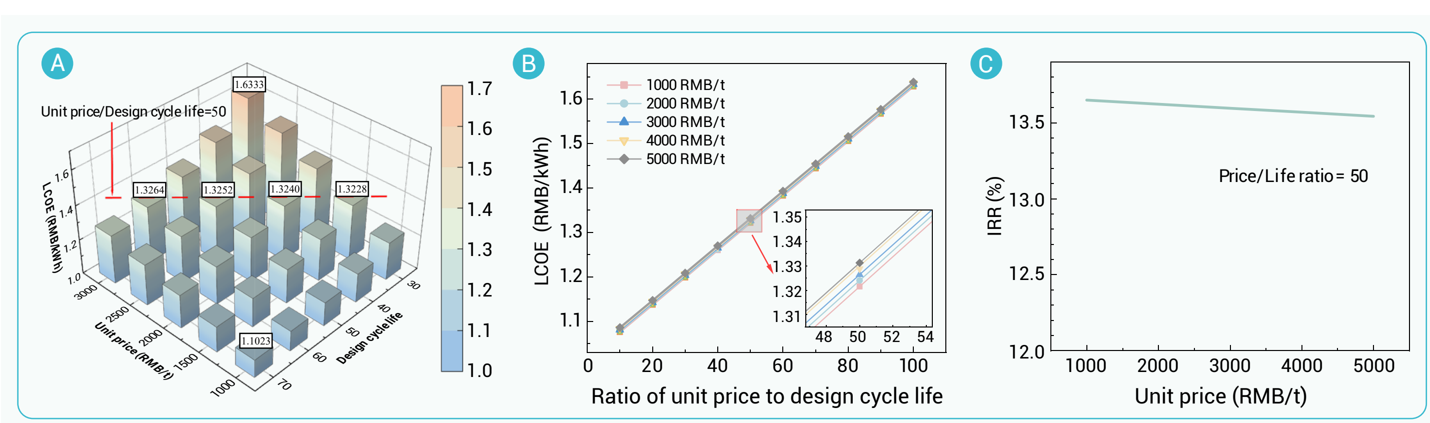

Figure 4. mpact of energy storage material cost and cycle life on the economic performance of the Carnot battery system (A) LCOE variations under different material unit prices and design cycle lives; (B) LCOE as a function of the ratio of unit price to design cycle life; (C) IRR as a function of material unit price.

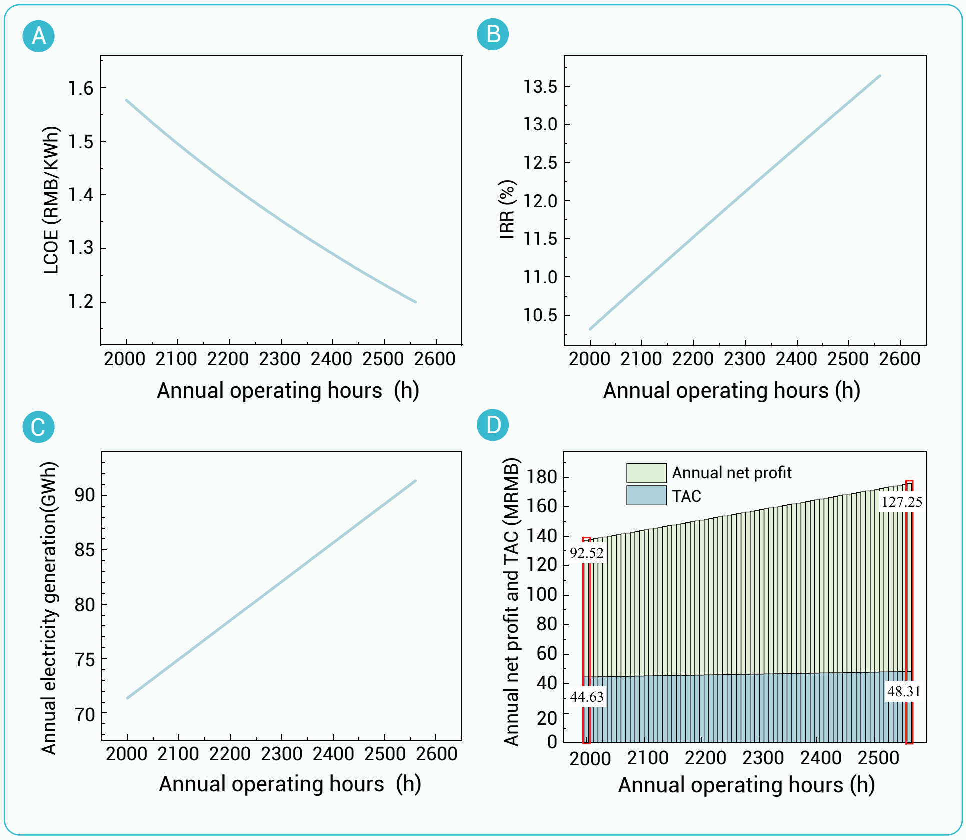

Figure 5. Impact of annual operating hours on techno-economic indicators (A) LCOE, (B) IRR, (C) Annual electricity generation, (D) Annual net profit and TAC.

evidenced by the red trendline in Figure 4A. However, it is noteworthy that for identical Price/Life ratios of 50, LCOE exhibits a slight but consistent increase as the absolute unit price rises. Figure 4B further demonstrates this trend: at fixed unit prices, the LCOE increases with a rising Price/Life ratio. The growth trajectories remain nearly identical across different unit prices, while increasing unit price alone elevates LCOE only marginally. This divergence indicates that although the Price/Life ratio is the primary determinant of LCOE, the initial material investment, governed by unit price, also exerts a secondary influence. Significantly, Figure 4C demonstrates that, with the Price/Life ratio held constant, increasing the energy storage material unit price from 1000 to 5000 RMB/t reduces the IRR by merely 0.11 percentage points – from 13.65% to 13.54%.

In summary, the analysis indicates that the Price/Life ratio is the primary factor influencing LCOE, while the initial material investment represented by unit price has a secondary but significant impact; concurrently, an increase in unit price exerts a slight negative effect on IRR.

as useful outputs, leading to an energy efficiency of 50.80%, with the remaining portion attributed to unavoidable heat losses in heat transfer processes and the power cycle.

In contrast, Figure 3B illustrates the corresponding exergy flow, which explicitly accounts for energy quality degradation along the conversion chain. Despite the large energy contribution from industrial waste heat, its exergy content is relatively limited due to its low temperature, resulting in a noticeable reduction in the useful exergy available to the system. The major sources of exergy destruction are observed in the BHP, the dehydration/hydration reactors, and the power block, where significant irreversibilities arise from electricity-to-heat conversion, chemical reaction processes, and finite temperature differences in the heat exchanger network. As a result, the overall exergy efficiency is reduced to 38.68%, which is substantially lower than the corresponding energy efficiency. This discrepancy highlights the thermodynamic penalty associated with multi-stage energy conversion and underlines the importance of high-temperature operation and improved heat integration to mitigate exergy destruction.

Effects of material cost and durability

To investigate the impact of material cost and durability on system economics, hypothetical scenarios for energy storage materials were established across varying unit prices (RMB/t) and design cycle life (number of charge–discharge cycles to end-of-life), with the corresponding LCOE visualized in Figure 4A. The analysis of the data reveals that at a unit price of 1000 RMB/t, increasing the material design cycle life from 30 to 70 cycles leads to a reduction in the LCOE from 1.219 RMB/kWh to 1.102 RMB/kWh, representing a 9.59% decrease. Notably, the sensitivity of LCOE to cycle life intensifies significantly at higher material costs. For instance, when the unit price rises to 3000 RMB/t, the same extension from 30 to 70 cycles yields a substantially greater 21.47% reduction in LCOE. This pronounced amplification underscores the critical dependence of high-cost energy storage materials on extended cycle performance to achieve economically viable levelized energy costs.

Furthermore, analysis of the data reveals a strong positive correlation between LCOE and the ratio of unit price to design cycle life (Price/Life), as

Effect of annual operating hours

Annual operating hours, defined as the total yearly duration of energy dispatch cycles, critically influence the techno-economic performance of Carnot battery systems. Figure 5 shows the sensitivity analysis of annual operating hours on system performance. Specifically, as operational duration increases from 2000 to 2560 hours, the LCOE exhibits a pronounced declining trend, as quantified in Figure 5A, decreasing from 1.577 RMB/kWh to 1.200 RMB/kWh. This reduction is attributed to the allocation of greater regenerated electricity output over fixed capital costs. Concurrently, the IRR demonstrates a robust positive correlation with annual operating hours, rising from 10.32% to 13.64% as shown in Figure 5B, indicating enhanced financial viability under extended operation.

Further analysis demonstrates the critical role of annual operating hours in affecting regenerated electricity, operating costs, and net profitability. As shown in Figure 5C, annual regenerated electricity output increases linearly with operating hours, rising from 71.37 GWh to 91.35 GWh — the primary driver of annual revenue. Concurrently, Figure 5D reveals that the TAC exhibits only a modest increase from 44.63 MRMB to 48.31 MRMB. This limited cost escalation stems from labor and equipment maintenance expenses being calculated based on maximum annual operating capacity, whereas only material consumption costs fluctuate with actual operating time. Consequently, revenue growth substantially outpaces the marginal rise in TAC, demonstrating the economic benefit of maximizing operating hours within technically feasible limits.

Scaling effects

Similarly, the economic viability of the Carnot battery system coupled with thermochemical storage exhibits a pronounced dependence on its installed capacity. A comprehensive sensitivity analysis, spanning system scales from 10 MW to 50 MW, reveals consistent and significant scaling effects across all major techno-economic indicators, as detailed in Figure 6.

Significantly, cost metrics demonstrate substantial improvements with increasing scale. As shown in Figure 6A, the Levelized Cost of Electricity exhibits a strong downward trend, declining from 2.233 RMB/kWh at 10 MW to 1.200 RMB/kWh at 50 MW. This reduction is intrinsically linked to the

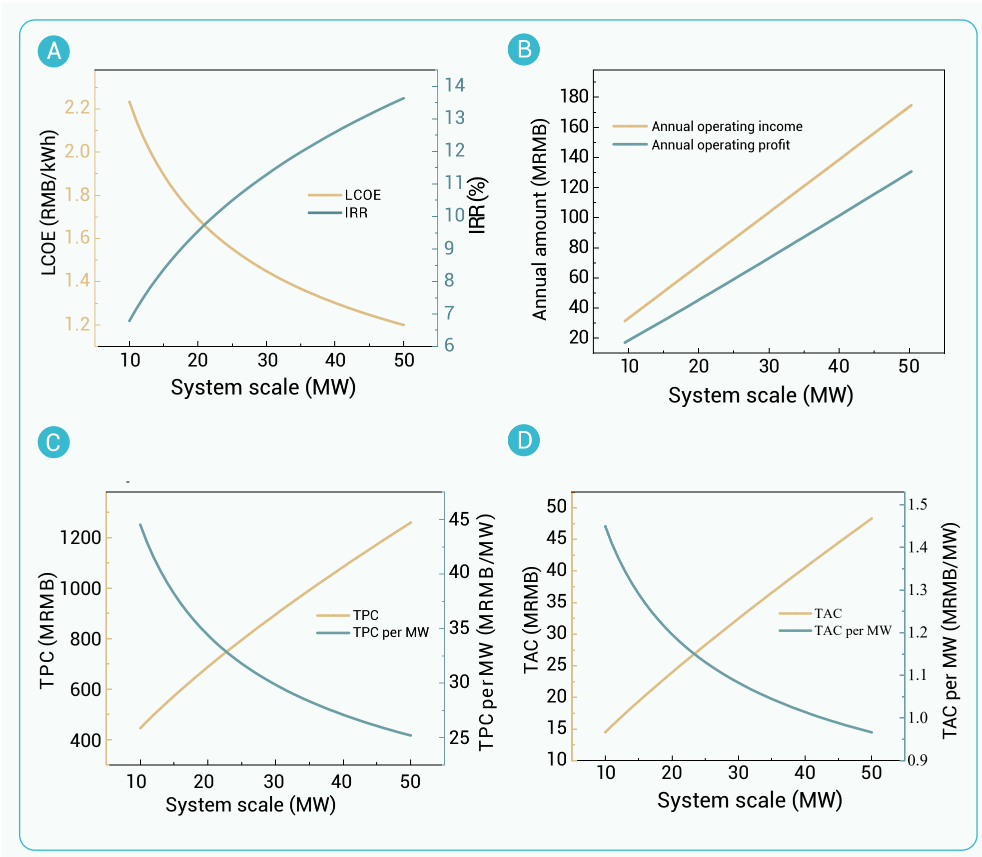

Figure 6. Evolution of key techno-economic indicators for the Carnot battery system across scaling capacities from 10 MW to 50 MW (A) LCOE and IRR, (B) Annual operating income and Annual operating profit, (C) TPC and TPC per MW, (D) TAC and TAC per MW.

favorable scaling of capital investments, as evidenced by Figure 6C, which shows that while the TPC increases nominally with capacity, the critical metric of TPC per MW reveals significant economies of scale, decreasing from 44.52 MRMB/MW at 10 MW to 25.19 MRMB/MW at 50 MW. Similarly, Figure 6D demonstrates that the TAC per MW undergoes a marked reduction, declining from 1.45 MRMB/MW at 10 MW to 0.97 MRMB/MW at 50 MW. This progressive decline in specific costs underscores the system's inherent potential for improved economic efficiency at larger installations.

Concurrently, financial return and operational performance metrics exhibit positive scaling correlations. As depicted in Figure 6A, the IRR experiences a steady increase, rising from 6.79% at 10 MW to 13.64% at 50 MW, reflecting enhanced project profitability at larger scales. Operational financial outputs strengthen considerably. Figure 6B illustrates substantial growth in annual operating income, escalating from 35.11 MRMB at 10 MW to 175.56 MRMB at 50 MW. This growth is mirrored, albeit with a different gradient, in the annual operating profit shown in Figure 6B, which increases from 20.62 MRMB to 127.25 MRMB across the investigated capacity spectrum. Such improvements stem from the system's ability to leverage larger capacities for greater revenue generation while benefiting from the per-unit cost reductions described earlier.

These observed trends collectively highlight the significant economies of scale within the proposed Carnot battery system. These economies of scale are primarily driven by the dilution of fixed capital investment, the relatively slow increase in operating costs, and the substantial growth in electricity generation and revenue with increasing system capacity. This scaling effect indicates that capacities towards the upper end of the analyzed range, particularly between 35 MW and 50 MW, offer substantially sperior economics. The convergence of decreasing LCOE, increasing IRR, and growing operational profits establishes a clear pathway towards improved economic sustainability with scale. These findings provide vital quantitative benchmarks for cost-optimized deployment of thermochemical Carnot battery systems.

Impact of electricity price dynamics on system economics

The economic viability of the Carnot battery system critically depends on electricity price dynamics, particularly the charging cost from curtailed renewable energy and the discharge price. The sensitivity of key economic indicators to these price variables was rigorously analyzed, as detailed in Figure 7.

As shown in Figure 7A, LCOE exhibits a direct and positive correlation with the net charging cost per kWh (hereafter referred to as net charging cost), which comprehensively considers factors such as electricity pricing and energy storage for peak shaving. As the net charging cost decreases, for instance when energy storage generates revenue during negative electricity price periods, the LCOE significantly declines. This underscores the substantial economic advantage of accessing low-cost or negatively priced curtailed wind and solar power for charging. Conversely, a positive net charging cost, which indicates potential grid injection costs or other expenses, elevates the LCOE, directly impacting the baseline competitiveness of the stored energy.

As depicted in Figure 7B, the project's financial attractiveness, measured by the IRR, demonstrates high sensitivity to both price components. Crucially, the discharge electricity price exerts a dominant positive influence on IRR, higher peak discharge tariffs dramatically improve project returns. While a lower (more negative) net charging cost also boosts IRR, its relative impact magnitude is generally secondary compared to the discharge price. This analysis underscores that ensuring high discharge rates during peak periods is paramount for achieving attractive investment returns, especially when stored electricity incurs additional charging costs. Conversely, in scenarios featuring negative electricity prices or zero-cost charging from curtailed wind and solar power, relatively low peak discharge prices can still sustain high internal rates of IRR. This enables relaxing strict requirements for charge/discharge timing, thereby achieving higher annual operational hours.

The Dynamic Payback Period (DPP) is similarly sensitive to the electricity price dynamics, particularly the spread between discharge price and charging cost. Figure 7C demonstrates that a higher discharge price coupled with a lower (more negative) net charging cost synergistically shortens the DPP, accelerating capital recovery. For instance, under a net charging cost of -0.100 RMB/kWh, increasing the discharge price from 1.100 RMB/kWh to 1.800 RMB/kWh reduces the DPP from approximately 27 years to around 12 years. This inverse relationship emphasizes that favorable price arbitrage conditions are essential for mitigating investment risk through faster payback.

Finally, the Annual net profit provides a clear picture of operational profitability under varying price regimes, as evidenced by Figure 7D, which shows that the profitability is highly responsive to increases in the discharge price. This result solidifies the economic model underpinning the Carnot battery system: profitability hinges fundamentally on the ability to capitalize on price differentials—charging economically using low-cost or incentivized curtailed energy and discharging strategically during high-price periods.

In conclusion, the economic performance of the Carnot battery system is profoundly sensitive to the dynamics of electricity prices. Accessing negatively priced or very low-cost curtailed renewable energy provides a crucial foundation for reducing LCOE and improving overall economics. However, the system's financial success, reflected in IRR, DPP, and Annual net profit, is predominantly governed by how the system adjusts its charging and

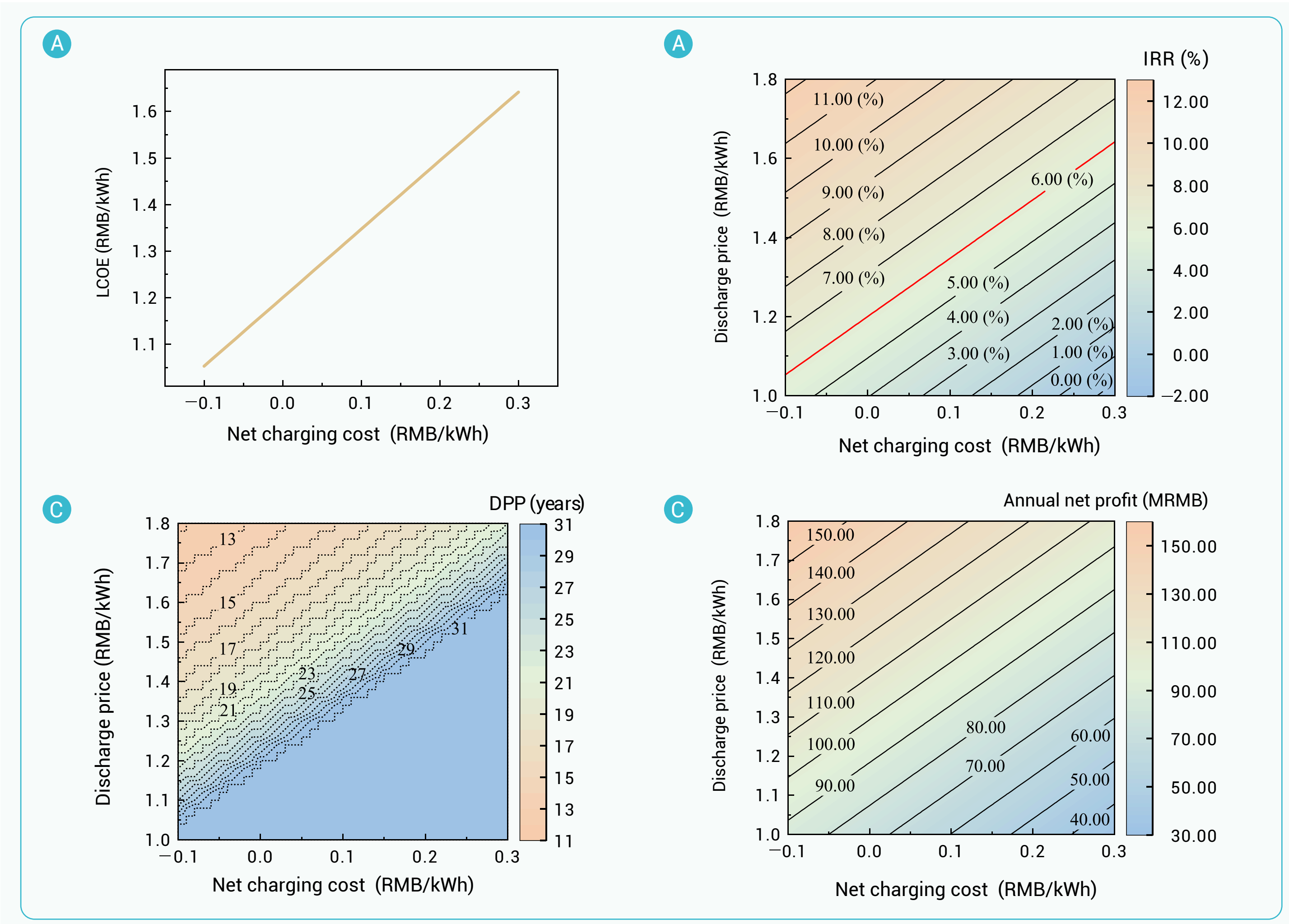

Figure 7. Sensitivity of economic indicators to electricity price dynamics (A) LCOE vs. net charging cost from curtailment, (B) IRR vs. net charging cost and discharge price, (C) DPP vs. net charging cost and discharge price, (D) Annual profit vs. concurrent charging cost and discharge price.

discharging operations to follow electricity pricing policies, thereby securing low charging costs while discharging during peak pricing periods.

CONCLUSIONS

The decarbonization of global energy systems necessitates efficient LDES solutions to address renewable intermittency. This study proposed and optimized a novel Carnot battery system integrating $Ca(OH)_2/CaO$ TCES, S-CO_2 BHP and BP, and industrial waste heat recovery. Multi-objective optimization employing the NSGA-II algorithm and HEATSEP framework achieved a round-trip efficiency of 67.95% and LCOE of 1.200 RMB/kWh at the 50 MW scale, significantly surpassing conventional Carnot batteries and demonstrating high technical feasibility. This performance level exceeds that of conventional Carnot battery systems, which typically exhibit round-trip efficiencies in the range of 40–60%. Furthermore, compared with hydrogen energy storage and power-to-gas pathways, the proposed system demonstrates advantages in economic performance, operational safety, and deployment flexibility. Compared with compressed air energy storage systems, which typically achieve round-trip efficiencies of 45–70% and require site-specific underground storage, the proposed system offers comparable efficiency with greater deployment flexibility. Moreover, because CAES follows an electric-to-electric pathway, this technology holds development potential in the thermal storage field.

Economically, the scale effects significantly enhance system viability: expanding from 10 MW to 50 MW reduces the LCOE by 46.3% and doubles the IRR to 13.64%. This is primarily due to a 44% reduction in specific investment and a 33% decrease in operational costs per MW. Additionally, maximizing the annual operating hours to 2,560 further improves the system's economic performance, as net profits substantially increase with longer operational periods. The economics of storage materials are primarily driven by the Price/Life ratio, with cycle life extensions having the most considerable impact on high-cost materials. At a unit price of 3,000 RMB/t, LCOE is reduced by 21.47% when increasing life from 30 to 70 cycles. The combined influence of material cost and cycle performance on system economics provide valuable benchmarks for energy storage material development.

Commercially, profitability is fundamentally driven by electricity price arbitrage and energy storage economic policies. Discharge prices, with their greater volatility, play a dominant role in financial returns. The dynamic payback period can reduce to approximately 12 years under favorable discharge pricing exceeding 1.800 RMB/kWh and negative charging costs. Therefore, regional deployment should prioritize high price-differential markets, leveraging strategic dispatch during low-cost charging and high-value discharge periods to ensure rapid capital recovery. In contrast, the system may not exhibit favorable economics in low price-differential markets due to high capital costs. Future work should explore diverse power cycles or coupling with coal-fired power plants to reduce capital costs and improve economic viability across a broader range of market scenarios.

REFERENCES

1. Yang J., Xu Q., Kou X., et al. (2024). Three-dimensional pore-scale study of methane hydrate dissociation mechanisms based on micro-CT images. *Innov. Energy* **1**:100015. DOI:10.59717/j.xinn-energy.2024.100015
2. Cherp A., Vinichenko V., Tosun J., et al. (2021). National growth dynamics of wind and solar power compared to the growth required for global climate targets. *Nat. Energy*

6:742–754. DOI:10.1038/s41560-021-00863-0
3. Chacartegui R., Alovisio A., Ortiz C., et al. (2016). Thermochemical energy storage of concentrated solar power by integration of the calcium looping process and a CO_2 power cycle. *Appl. Energy* 173:589–605. DOI:10.1016/j.apenergy.2016.04.053
4. Denholm P., Arent D. J., Baldwin S. F., et al. (2021). The challenges of achieving a 100% renewable electricity system in the United States. *Joule* 5:1331–1352. DOI:10.1016/j.joule.2021.03.028
5. Staadecker M., Szinai J., Sánchez-Pérez P. A., et al. (2024). The value of long-duration energy storage under various grid conditions in a zero-emissions future. *Nat. Commun.* 15:9501. DOI:10.1038/s41467-024-53274-6
6. Chun S.-E., Evanko B., Wang X., et al. (2015). Design of aqueous redox-enhanced electrochemical capacitors with high specific energies and slow self-discharge. *Nat. Commun.* 6:7818. DOI:10.1038/ncomms8818
7. Luo X., Wang J., Dooner M., et al. (2015). Overview of current development in electrical energy storage technologies and the application potential in power system operation. *Appl. Energy* 137:511–536. DOI:10.1016/j.apenergy.2014.09.081
8. Lund P. D., Lindgren J., Mikkola J., et al. (2015). Review of energy system flexibility measures to enable high levels of variable renewable electricity. *Renew. Sustain. Energy Rev.* 45:785–807. DOI:10.1016/j.rser.2015.01.057
9. Raju M. and Kumar Khaitan S. (2012). Modeling and simulation of compressed air storage in caverns: A case study of the Huntorf plant. *Appl. Energy* 89:474–481. DOI:10.1016/j.apenergy.2011.08.019
10. Zakeri B. and Syri S. (2015). Electrical energy storage systems: A comparative life cycle cost analysis. *Renew. Sustain. Energy Rev.* 42:569–596. DOI:10.1016/j.rser.2014.10.011
11. Zhao A. P., Li S., Xie D., et al. (2025). Hydrogen as the nexus of future sustainable transport and energy systems. *Nat. Rev. Electr. Eng.* 2:447–466. DOI:10.1038/s44287-025-00178-2
12. Dawood F., Anda M. and Shafiullah G. M. (2020). Hydrogen production for energy: An overview. *Int. J. Hydrogen Energy* 45:3847–3869. DOI:10.1016/j.ijhydene.2019.12.059
13. Götz M., Lefebvre J., Mörs F., et al. (2016). Renewable Power-to-Gas: A technological and economic review. *Renew. Energy* 85:1371–1390. DOI:10.1016/j.renene.2015.07.066
14. Gibb B. C. (2025). Carnot batteries for dispatchable renewables. *Nat. Chem.* 17:629–631. DOI:10.1038/s41557-025-01813-z
15. Zhang C., Li M., Dang C., et al. (2025). Enhanced Carnot battery for high-efficiency energy storage: Feasibility analysis. *Energy Conver. Manag.* 332:119754. DOI:10.1016/j.enconman.2025.119754
16. Vecchi A., Knobloch K., Liang T., et al. (2022). Carnot Battery development: A review on system performance, applications and commercial state-of-the-art. *J. Energy Stor.* 55:105782. DOI:10.1016/j.est.2022.105782
17. Olympios A., McTigue J., Antunez P., et al. (2021). Progress and Prospects of Thermo-Mechanical Energy Storage - A Critical Review. *Progress in Energy.*
18. Benato A. (2017). Performance and cost evaluation of an innovative Pumped Thermal Electricity Storage power system. *Energy* 138:419–436. DOI:10.1016/j.energy.2017.07.066
19. Jockenhöfer H., Steinmann W.-D. and Bauer D. (2018). Detailed numerical investigation of a pumped thermal energy storage with low temperature heat integration. *Energy* 145:665–676. DOI:10.1016/j.energy.2017.12.087
20. Qiao H., Yu X. and Yang B. (2023). Working fluid design and performance optimization for the heat pump-organic Rankine cycle Carnot battery system based on the group contribution method. *Energy Conver. Manag.* 293:117459. DOI:10.1016/j.enconman.2023.117459
21. Sciacovelli A., Vecchi A. and Ding Y. (2017). Liquid air energy storage (LAES) with packed bed cold thermal storage – From component to system level performance through dynamic modelling. *Appl. Energy* 190:84–98. DOI:10.1016/j.apenergy.2016.12.118
22. Borri E., Tafone A., Romagnoli A., et al. (2017). A preliminary study on the optimal configuration and operating range of a "microgrid scale" air liquefaction plant for Liquid Air Energy Storage. *Energy Conver. Manag.* 143:275–285. DOI:10.1016/j.enconman.2017.03.079
23. Kantharaj B., Garvey S. and Pimm A. (2015). Compressed air energy storage with liquid air capacity extension. *Appl. Energy* 157:152–164. DOI:10.1016/j.apenergy.2015.07.076
24. Linares J. I., Montes M. J., Cantizano A., et al. (2020). A novel supercritical CO_2 recompression Brayton power cycle for power tower concentrating solar plants. *Appl. Energy* 263:114644. DOI:10.1016/j.apenergy.2020.114644
25. Tesio U., Guelpa E. and Verda V. (2020). Integration of thermochemical energy storage in concentrated solar power. Part 2: Comprehensive optimization of supercritical CO_2 power block. *Energy Conver. Manag. X* 6:100038. DOI:10.1016/j.ecmx.2020.100038
26. Ortiz C., García-Luna S., Carro A., et al. (2024). Techno-economic analysis of a modular thermochemical battery for electricity storage based on calcium-looping. *Appl. Energy* 367:123366. DOI:10.1016/j.apenergy.2024.123366
27. Xu Q., Wang I., Li Z., et al. (2023). A calcium looping system powered by renewable electricity for long-term thermochemical energy storage, residential heat supply and carbon capture. *Energy Conver. Manag.* 276:116592. DOI:10.1016/j.enconman.2022.116592
28. Wang D., Sun Z., Xu Q., et al. (2024). Thermodynamic modeling and analysis of a Carnot battery system integrating calcium looping thermochemical energy storage with coal-fired power plant. *Energy Conver. Manag.* 318:118888. DOI:10.1016/j.enconman.2024.118888
29. Liu H., Zhang Y., Xu Q., et al. (2025). A Carnot battery system integrating $Ca(OH)_2$/CaO thermochemical energy storage and supercritical CO_2 cycles for long-term energy storage and residential heat supply. *Appl. Energy* 377:124535. DOI:10.1016/j.apenergy.2024.124535
30. Xu B., Li P. and Chan C. (2015). Application of phase change materials for thermal energy storage in concentrated solar thermal power plants: A review to recent developments. *Appl. Energy* 160:286–307. DOI:10.1016/j.apenergy.2015.09.016
31. Dai L., Long X.-F., Lou B., et al. (2018). Thermal cycling stability of thermochemical energy storage system $Ca(OH)_2$/CaO. *Appl. Therm. Eng.* 133:261–268. DOI:10.1016/j.applthermaleng.2018.01.059
32. Morgenstern L., Talebi E., Kerscher F., et al. (2023). Experimental investigation of CaO/$Ca(OH)_2$ for thermochemical energy storage – commissioning of a 0.5 kWh experimental setup. *Fuel* 345:128220. DOI:10.1016/j.fuel.2023.128220
33. Zhang Y., Liu H., Lu J., et al. (2025). An integrated energy storage system coupling Ca(OH)2/CaO/CaCO3 thermochemical energy storage, supercritical CO2 cycle, and CO2 capture. *J. Energy Stor.* 130:117487. DOI:10.1016/j.est.2025.117487
34. Weiland N. T., Lance B. W. and Pidaparti S. R. (2019). sCO_2 Power Cycle Component Cost Correlations From DOE Data Spanning Multiple Scales and Applications. *ASME* 9. DOI:10.1115/GT2019-90493

FUNDING AND ACKNOWLEDGMENTS

This research was supported by the National Key Research and Development Program of China (No.2024YFE0212800) and National Natural Science Foundation of China (Nos.52090062, 52206014 and U22B20112) and Basic Research Foundation of Xi'an Thermal Power Research Institute Co., Ltd.(No. TA-25-TYK68). Academic Papers of the 28th Annual Meeting of the China Association for Science and Technology.

AUTHOR CONTRIBUTIONS

Huawei Liu: Conceptualization, Methodology, Software, Investigation, Data curation, Visualization. Yongqing Zhang: Formal analysis, Investigation, Data curation, Validation, Visualization, Writing – original draft, Writing – review & editing. Qianghui Xu: Conceptualization, Resources, Supervision, Project administration, Funding acquisition, Methodology, Writing – review & editing. Wei Han: Investigation, Resources. Kezhen Zhang: Investigation, Resources. Xiao Yang: Data curation, Visualization. Chenglong Yang: Investigation, Data curation, Validation. Sheng Li: Resources, Supervision, Project administration. Jun Shen: Resources, Supervision, Funding acquisition, Writing – review & editing. All authors have read and approved the final version of the manuscript. All authors contributed to the manuscript and approved the final version.

DECLARATION OF INTERESTS

Jun Shen is an Editorial Board member of The Innovation Energy and was blinded from reviewing or making final decisions on the manuscript. Peer review was handled independently of this member and their research group. The other authors declare no conflicts of interest.

DATA AND CODE AVAILABILITY

Data are available from the corresponding author upon reasonable request.